Dymore User's Manual

Formulation and finite element implementation of elastomeric devices

Contents

1 Classical linear viscoelasticity

This section reviews of basic concepts of linear viscoelasticity that will be used in the remainder of this work. Often, one-dimensional rheological models [1, 2] are used to introduce the concepts associated with viscoelasticity. Typically, these models involve serial or parallel combinations of linear or nonlinear springs and dashpots to form increasingly complex models. For instance, fig. 1 depicts the generalized Maxwell model. The spring elements characterize the elastic behavior of the material, whereas its energy dissipation characteristics are described by the dashpot elements. Mathematically, these models can be expressed as ordinary differential equations in time, often involving internal states, or through convolution integrals.

1.1 The generalized Maxwell model

The generalized Maxwell model depicted schematically in fig 1 consists of an elastic spring, the "elastic branch," in parallel with one or more Maxwell fluid elements, the "viscous branches." Assuming the device to be of unit area and length, forces and elongations can be identified with stresses and strains, respectively. The spring stiffness constants are denoted $E_\infty > 0$ and $E_b > 0$, $b = 1, \ldots, N_b$, where N_b is the number of Maxwell fluid elements. The dashpot constants are denoted $\eta_b > 0$, $b = 1, \ldots, N_b$.

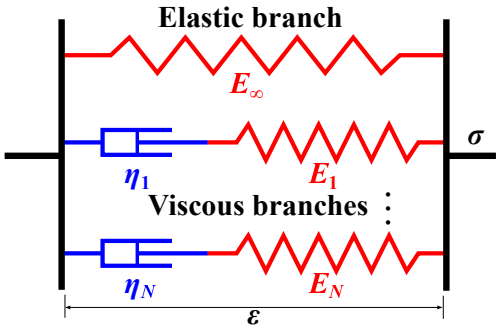

Figure 1: Schematic of the generalized Maxwell model.

Elementary mechanics yields the constitutive equations for the various components of the system. For the elastic branch, $\sigma_\infty = E_\infty \varepsilon$, where σ_∞ is the stress in the elastic branch and ε the strain of the device. The stress in a typical viscous branch is $\sigma_b = \eta_b \dot{\alpha}_b = E_b(\varepsilon - \alpha_b)$, where the first equation provides the constitutive equation for the dashpot, the second for the elastic spring, and α_b can be interpreted as the strain in the dashpot. Notation $\dot{(\cdot)}$ indicates a derivative with respect to time. Finally, the total stress, σ, is found by summing up the stresses in the branches, $\sigma = \sigma_\infty + \sum_{b=1}^{N_b} \sigma_b$. Introducing the constitutive relationships yields

$$\sigma = E_\infty \varepsilon + \sum_{b=1}^{N_b} E_b(\varepsilon - \alpha_b), \tag{1}$$

where variables α_b can be interpreted as internal states of the model.

Because the stresses in the spring and dashpot of each viscous branch are identical, $\eta_b \dot{\alpha}_b = E_b(\varepsilon - \alpha_b)$, and hence, the internal states must satisfy the following evolution equation

$$\tau_b \dot{\alpha}_b + \alpha_b = \varepsilon, \quad b = 1, 2, \ldots, N_b, \tag{2}$$

where the relaxation times, τ_b, are defined as

$$\tau_b = \frac{\eta_b}{E_b}. \tag{3}$$

The first-order differential evolution equation (2) must satisfy the following initial condition, $\lim_{t \to -\infty} \alpha_b = 0$.

Because the evolution equation (2) can be recast as $\mathrm{d}[\exp(t/\tau_b)\alpha_b]/\mathrm{d}t = (1/\tau_b)\exp(t/\tau_b)\varepsilon$, integration over time yields $\alpha_b = (1/\tau_b)\int_{-\infty}^{t} \exp[-(t-s)/\tau_b]\varepsilon(s)\ \mathrm{d}s$. Assuming that $\varepsilon(t) \to 0$ as $t \to -\infty$, integration by parts then leads to

$$\alpha_b(t) = \varepsilon(t) - \int_{-\infty}^{t} e^{-(t-s)/\tau_b}\dot{\varepsilon}(s)\ \mathrm{d}s. \tag{4}$$

The stress convolution integral then follows from introducing eq. (4) into eq. (1) to find

$$\sigma(t) = \int_{-\infty}^{t} G(t-s)\dot{\varepsilon}(s)\ \mathrm{d}s, \tag{5}$$

where the relaxation function, $G(t)$, is defined as

$$G(t) = E_\infty + \sum_{b=1}^{N_b} E_b e^{-t/\tau_b}. \tag{6}$$

In summary, the generalized Maxwell model can be expressed by convolution integral (5), where the relaxation function is defined by eq. (6). Alternatively, the same model can be represented by eq. (1), where the internal variables satisfy the differential equations of evolution (2). These two formulations of the same model will be used in the sequel.

Note that for $N_b = 0$, the relaxation function reduces to $G(t) = E_\infty$ and eq. (5) then simplifies to $\sigma(t) = E_\infty\varepsilon(t)$, *i.e.*, linear elasticity is recovered. Clearly, the first term of the relation function models the linearly elastic behavior of the material and each of the terms under the summation sign characterize viscoelastic behavior with a material time constant, τ_b. The same observation can be made for the evolution equations: if $\tau_b = 0$, the solution of evolution equation (2) is $\alpha_b = \varepsilon$, and eq. (1) yields $\sigma = E_\infty\varepsilon$, as expected.

1.2 Alternative formulation

In the previous section, two formulations of the generalized Maxwell model were presented: the first is based on differential equations of evolution and the second on a convolution integral. From a computational point of view, the differential equation of evolution approach is easier to implement. In this section, two variations of the differential equations of evolution approach are presented.

The first approach is summarized by eqs. (1) and (2), repeated here for convenience,

$$\sigma = E_\infty\varepsilon + \sum_{b=1}^{N_b} E_b(\varepsilon - \alpha_b), \tag{7a}$$

$$\tau_b\dot{\alpha}_b + \alpha_b = \varepsilon, \quad b = 1, 2, \ldots, N_b. \tag{7b}$$

When the system reaches equilibrium, *i.e.*, when $\dot{\alpha}_b \approx 0$, the internal variables of the system all become equal to the strain, $\alpha_b \approx \varepsilon$ and eq. (7a) reduces to $\sigma = E_\infty\varepsilon$. This observation justifies the subscript $(\cdot)_\infty$ used for the spring stiffness constant of the elastic branch: if the system is brought to equilibrium for $t \to \infty$, its stiffness is E_∞.

1.2.1 Alternative internal variable

Equation (7a) can be recast as $\sigma = E_0\varepsilon - \sum_{b=1}^{N_b} E_b\alpha_b$, where

$$E_0 = E_\infty + \sum_{b=1}^{N_b} E_b. \tag{8}$$

Denoting $s_b = E_b\alpha_b$ now leads to $\sigma = E_0\varepsilon - \sum_{b=1}^{N_b} s_b$ and multiplication of eq. (7b) by E_b yields $\tau_b\dot{s}_b + s_b = E_b\varepsilon$. Model (7) is now recast as

$$\sigma = E_0\varepsilon - \sum_{b=1}^{N_b} s_b, \tag{9a}$$

$$\tau_b\dot{s}_b + s_b = \nu_b E_0\varepsilon, \quad b = 1, 2, \ldots, N_b. \tag{9b}$$

The following parameters were introduced

$$\nu_\infty = \frac{E_\infty}{E_0}, \quad \nu_b = \frac{E_b}{E_0}, \quad \nu_\infty + \sum_{b=1}^{N_b} \nu_b = 1. \tag{10}$$

In summary, the following equations provide an alternative formulation of the model proposed by Simo and Hughes [3],

$$\sigma = \frac{\mathrm{d}A(\varepsilon)}{\mathrm{d}\varepsilon} - \sum_{b=1}^{N_b} s_b, \tag{11a}$$

$$\tau_b\dot{s}_b + s_b = \nu_b\frac{\mathrm{d}A(\varepsilon)}{\mathrm{d}\varepsilon}, \quad b = 1, 2, \ldots, N_b. \tag{11b}$$

This model introduces the strain energy of the system, $A(\varepsilon)$. For a quadratic strain energy, $A(\varepsilon) = 1/2\, E_0\varepsilon^2$, models (9) and (11) are identical. The latter model, however, can be extended to nonlinear elastic materials by selecting a more general expression for the strain energy.

In this alternative formulation, the internal variables of the model, $s_b = E_b\alpha_b$, are used in place of variables α_b. The latter variables represent the stretches in the dashpots, but the physical interpretation of the former is not as clear. The evolution equations for both sets of variables, see eq. (9b) and (11b), are similar.

1.3 Time domain description of relaxation function

Equation (5) describes the behavior of viscoelastic materials in the time domain when subjected to a strain history, $\varepsilon(t)$. The response of the material is characterized by the relaxation function, $G(t)$, which can be interpreted as the time-dependent stiffness matrix of the material. In the generalized Maxwell model, the relaxation function is expanded in Prony series, see eq. (6).

Hence, the physical interpretation of the relaxation function can be obtained easily. Consider a step input in strain history, $\varepsilon(t) = 0$ for $t < 0$, and $\varepsilon(t) = \varepsilon_0$ for $t \geq 0$. Introducing this strain history in eq. (5) yields

$$\varepsilon(t) = \int_{-\infty}^{t} G(t-s)\dot{\varepsilon}(s)\, \mathrm{d}s = G(t)\varepsilon_0. \tag{12}$$

Clearly, the relaxation function describes the stress history after the application of the step input in strain. The instantaneous stiffness at time $t = 0$ is $E_0 = E_\infty + \sum_{b=1}^{N_b} E_b$, whereas the long-term, steady stiffness matrix is E_∞ when $t \to \infty$.

In practice, material viscoelastic properties can be obtained from a stress relaxation experiment: a strain step input is applied to the material and the measurement of the resulting stress provides the stress relaxation function. Curve fitting techniques are then used to extract Prony series from the experimental data.

1.4 Frequency domain description of relaxation function

In contrast to the time domain characterization described in the previous section, viscoelastic material can also be described in the frequency domain. Consider the following harmonic strain input,

$$\varepsilon(t) = \hat{\varepsilon} e^{i\Omega t}, \tag{13}$$

where $\hat{\varepsilon}$ is the amplitude of the harmonic excitation, Ω the excitation frequency and $i = \sqrt{-1}$. The internal state of branch b is expected to respond harmonically, $\alpha_b(t) = \hat{\alpha}_b \exp(i\Omega t)$, where the amplitude of the response, $\hat{\alpha}_b$, is a complex number. Introducing these expressions into evolution equation (2) yields

$$\alpha_b(t) = \frac{exp(-i\Omega\tau_b)}{\sqrt{1+(\Omega\tau_b)^2}}\varepsilon(t). \tag{14}$$

The total stress in the device then follows from eq. (1)

$$\sigma(t) = \left[E_\infty + \sum_{b=1}^{N_b} E_b \frac{(\Omega\tau_b)^2 + i(\Omega\tau_b)}{1+(\Omega\tau_b)^2}\right]\varepsilon(t). \tag{15}$$

It is customary to characterize the harmonic response of the material in terms of the *storage* or *elastic modulus* and *loss modulus*, denoted $G_e(\Omega)$ and $G_d(\Omega)$, respectively,

$$\sigma(t) = \left[G_e(\Omega) + iG_d(\Omega)\right]\varepsilon(t), \tag{16}$$

where $[G_e(\Omega) + iG_d(\Omega)]$ is called the *complex modulus* of the material. The elastic and loss moduli characterize the in-phase and out-of-phase stress response. Identifying eqs. (15) and (16) then leads to

$$G_e(\Omega) = E_\infty + \sum_{b=1}^{N_b} E_b \frac{(\Omega\tau_b)^2}{1+(\Omega\tau_b)^2}, \tag{17a}$$

$$G_d(\Omega) = \sum_{b=1}^{N_b} E_b \frac{(\Omega\tau_b)}{1+(\Omega\tau_b)^2}. \tag{17b}$$

It is also common to characterize the complex modulus as an amplitude and a phase

$$G_e(\Omega) + iG_d(\Omega) = \sqrt{G_e^2 + G_d^2}e^{iG_d/G_e}. \tag{18}$$

The stress response is written as $\sigma(t) = \hat{\sigma}\exp[i(\Omega t + \phi)]$ and

$$\frac{\hat{\sigma}}{\hat{\varepsilon}} = \sqrt{G_e^2 + G_d^2}, \tag{19a}$$

$$\phi = \arctan\frac{G_d}{G_e}. \tag{19b}$$

The energy dissipated in the dashpot of branch b over one period is evaluated easily as

$$W_b^d = \int_0^T \eta_b \dot{\alpha}_b^2 \, \mathrm{d}t = \int_0^T \eta_b \frac{\Omega^2 \sin^2\Omega(t-\tau_b)}{1+(\Omega\tau_b)^2}\hat{\varepsilon}^2 \, \mathrm{d}t = \frac{\eta_b\Omega^2\hat{\varepsilon}^2}{1+(\Omega\tau_b)^2}\frac{T}{2}, \tag{20}$$

where $T = 2\pi/\Omega$ is the period of oscillation of the system. The energy dissipated by all dashpots, denoted W_d, becomes

$$\frac{W_d}{\pi\hat{\varepsilon}^2} = \sum_{b=1}^{N_b} E_b \frac{(\Omega\tau_b)}{1+(\Omega\tau_b)^2} = G_d(\Omega), \tag{21}$$

where the second equality follows from eq. (17b). This result implies the following observation: within a constant, the loss modulus equals the energy dissipated by the device over one period of oscillation.

1.5 The Kelvin-Voigt element

The Kelvin-Voigt element, depicted schematically in fig. 2 consists of an elastic spring of constant E, and a dashpot of constant η arranged in parallel. The constitutive laws for the two components are $\sigma_e = E\varepsilon$ and $\sigma_v = \eta\dot{\varepsilon}$, where σ_e and σ_v are the stresses in the spring and dashpot, respectively. The total stress in the Kelvin-Voigt element is now

$$\sigma = \sigma_e + \sigma_v = E\varepsilon + \eta\dot{\varepsilon}. \tag{22}$$

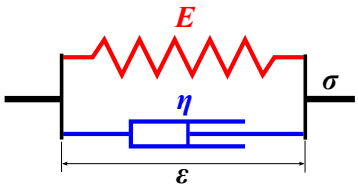

Figure 2: Schematic of the Kelvin-Voigt element.

The Kelvin-Voigt element is a particular case of the generalized Maxwell model with the following parameters: $N_b = 1$, $E_\infty = E$, $\tau_1 \to 0$ and $E_1 \to +\infty$ such that $E_1\tau_1 = \eta$.

With this set of parameters, eqs. (17) give the elastic and loss moduli of the Kelvin-Voigt element

$$\bar{G}_e(\Omega) = \frac{G_e(\Omega)}{E} = 1, \tag{23a}$$

$$\bar{G}_d(\Omega) = \frac{G_d(\Omega)}{E} = \Omega\tau, \tag{23b}$$

where $\tau = \eta/E$ is the relaxation time.

Figure 3 shows the non-dimensional elastic and loss moduli, defined by eqs. (23a) and (23b), respectively, as a function of the non-dimensional excitation frequency, $\Omega\tau$, on a logarithmic scale. Figure 4 shows the non-dimensional modulus and phase angle, defined by eqs. (19a) and (19b), respectively, as a function of the non-dimensional excitation frequency.

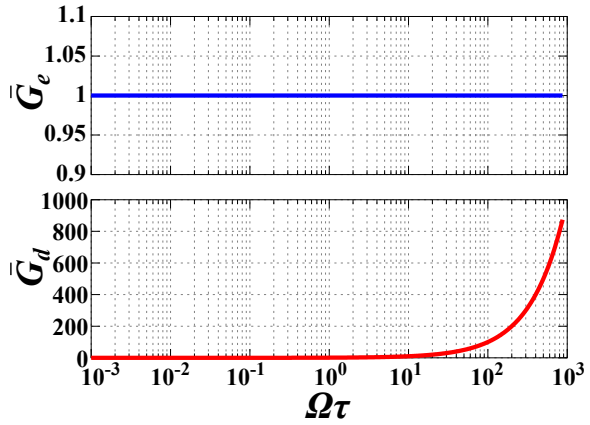

Figure 3: Non-dimensional elastic (top figure) and loss (bottom figure) moduli for the Kelvin-Voigt element versus non-dimensional frequency, $\Omega\tau$.

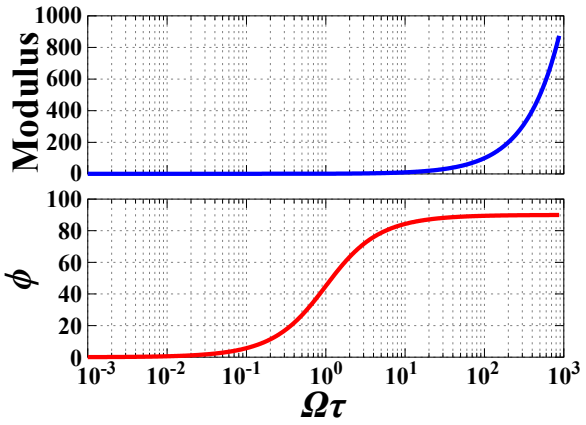

Figure 4: Non-dimensional loss modulus (top figure) and phase angle (bottom figure) for the Kelvin-Voigt element versus non-dimensional frequency, $\Omega\tau$.

Because the loss modulus can also be interpreted as the energy dissipated by the dashpot over one period, the data shown in fig. (3) implies the the energy dissipated by the Kelvin-Voigt element rises rapidly as the excitation frequency increases.

1.6 The Maxwell fluid element

Figure 5 depicts the Maxwell fluid element, which consists of an elastic spring of constant E and a dashpot of constant η arranged in series. Let $\alpha(t)$ denote the strain in the dashpot; the constitutive

laws for the two components are $\sigma = E(\varepsilon - \alpha)$ and $\sigma = \eta\dot{\alpha}$, where σ denotes the stress in the element. The governing equations for the Maxwell fluid element are now

$$\sigma = E(\varepsilon - \alpha), \tag{24a}$$

$$\tau\dot{\alpha} = \varepsilon - \alpha, \tag{24b}$$

where $\tau = \eta/E$ is the relaxation time. It is assumed that $\sigma = 0$ for $t \to -\infty$. The Maxwell fluid element is a particular case of the generalized Maxwell model with the following parameters: $N_b = 1$, $E_\infty = 0$, $E_1 = E$, $\tau_1 = \tau$.

With this set of parameters, eqs. (17) give the elastic and loss moduli of the Maxwell fluid element

$$\bar{G}_e(\Omega) = \frac{G_e(\Omega)}{E} = \frac{(\Omega\tau)^2}{1 + (\Omega\tau)^2}, \tag{25a}$$

$$\bar{G}_d(\Omega) = \frac{G_d(\Omega)}{E} = \frac{(\Omega\tau)}{1 + (\Omega\tau)^2}. \tag{25b}$$

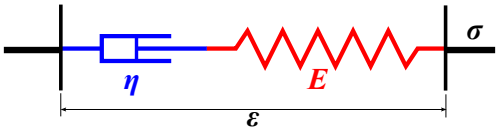

Figure 5: Schematic of the Maxwell fluid element

Figure 6 shows the non-dimensional elastic and loss moduli, defined by eqs. (25a) and (25b), respectively, as a function of the non-dimensional excitation frequency, $\Omega\tau$, on a logarithmic scale. Figure 7 shows the non-dimensional modulus and phase angle, defined by eqs. (19a) and (19b), respectively, as a function of the non-dimensional excitation frequency.

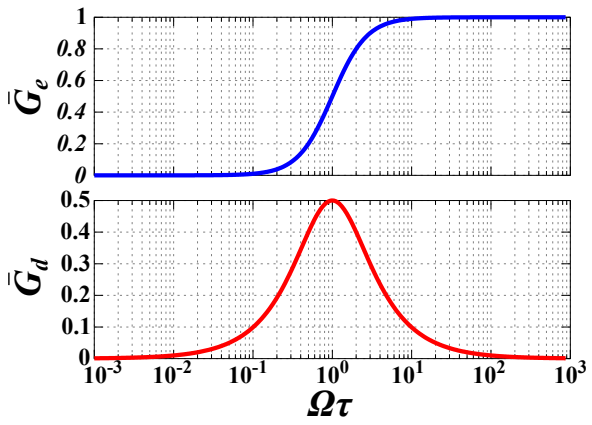

Figure 6: Non-dimensional elastic (top figure) and loss (bottom figure) moduli for the Maxwell fluid element versus non-dimensional frequency, $\Omega\tau$.

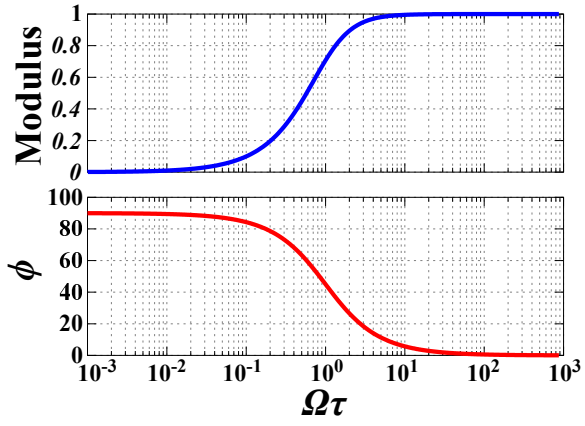

Figure 7: Non-dimensional loss modulus (top figure) and phase angle (bottom figure) for the Maxwell fluid element versus non-dimensional frequency, $\Omega\tau$.

Figure 6 shows that at low excitation frequencies, *i.e.*, when $\Omega\tau \to 0$, the elastic modulus of the Maxwell fluid element vanishes, as expected for a fluid. In contrast, the elastic modulus of the Kelvin-Voigt element is independent of frequency, see fig. 3.

The loss moduli of the Kelvin-Voigt and Maxwell fluid elements also differ sharply, as depicted in figs. 3 and 6. Note that the loss modulus of the Kelvin-Voigt element increases without bounds at high excitation frequencies, in contrast with that of the Maxwell fluid element, which shows a maximum for $\Omega\tau = 1$, then decreases at high frequencies. This latter behavior is that observed in actual materials.

Figure 8 compares the loss moduli of the Kelvin-Voigt and Maxwell fluid elements at low frequencies. Note that at low excitation frequencies, $\Omega\tau < 0.2$, the two loss moduli are in close agreement with each other. Consequently, the Kelvin-Voigt model should be used at low frequencies only.

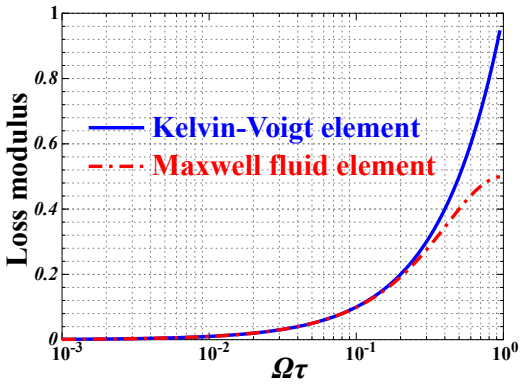

Figure 8: Comparison of the loss moduli of the Kelvin-Voigt and Maxwell fluid elements.

1.7 The Zener solid element

Figure 9 depicts the Zener solid element, which consists of an elastic spring of stiffness constant E_∞ and a Maxwell fluid element arranged in series. The Zener solid element, also known as the "linear solid element." The physical characteristics of the Maxwell fluid element are E_1 and η_1, as indicated in the figure. Let $\alpha(t)$ denote the strain in the dashpot. The governing equations for the Zener solid element become

$$\sigma = E_\infty \varepsilon + E_1(\varepsilon - \alpha), \tag{26a}$$

$$\tau\dot{\alpha} + \alpha = \varepsilon, \tag{26b}$$

where $\tau = \eta/E$ is the relaxation time. It is assumed that $\sigma = 0$ for $t \to -\infty$. The Zener solid element is a particular case of the generalized Maxwell model with a single viscoelastic branch.

With this set of parameters, eqs. (17) give the elastic and loss moduli of the Maxwell fluid element

$$\bar{G}_e(\Omega) = \frac{G_e(\Omega)}{E_0} = \frac{(1-\nu_1) + (\Omega\tau)^2}{1 + (\Omega\tau)^2}, \tag{27a}$$

$$\bar{G}_d(\Omega) = \frac{G_d(\Omega)}{E_0} = \frac{\nu_1(\Omega\tau)}{1 + (\Omega\tau)^2}, \tag{27b}$$

where $E_0 = E_\infty + E_1$ and $\nu_1 = E_1/E_0$.

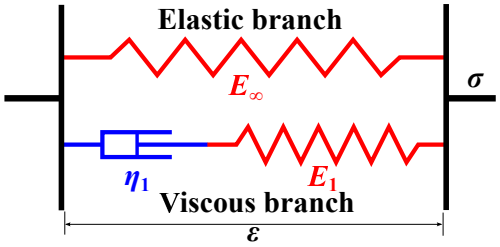

Figure 9: Schematic of the Maxwell element.

Figure 10 shows the non-dimensional elastic and loss moduli, defined by eqs. (27a) and (27b), respectively, as a function of the non-dimensional excitation frequency, $\Omega\tau$, on a logarithmic scale. Figure 11 shows the non-dimensional modulus and phase angle, defined by eqs. (19a) and (19b), respectively, as a function of the non-dimensional excitation frequency. For $\nu_1 = 1$, the Zener solid element degenerates into the Maxwell fluid element.

As was the case for the Maxwell fluid element, the loss modulus of the Zener solid element vanishes at both low and high frequencies, *i.e.*, when $(\Omega\tau) \to 0$ and $(\Omega\tau) \to \infty$. For the Zener solid element, low loss moduli are obtained for small values of its characteristic parameters, *i.e.*, for $\nu_1 \to 0$ and $\tau \to 0$.

1.8 The equivalent Zener solid element

As pointed out in section 1.6, the Kelvin-Voigt model in a low frequency approximation to the actual behavior of viscoelastic materials, see fig. 8. The present section addresses the following question: what are the parameters of a Zener solid element that will approximate the Kelvin-Voigt element in the low frequency range?

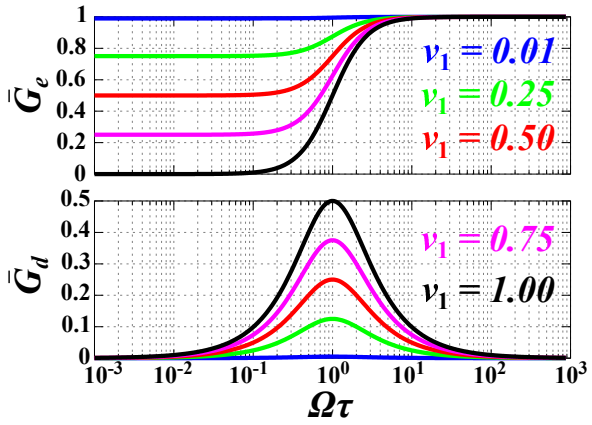

Figure 10: Non-dimensional elastic (top figure) and loss (bottom figure) moduli for the Zener solid element versus non-dimensional frequency, $\Omega\tau$.

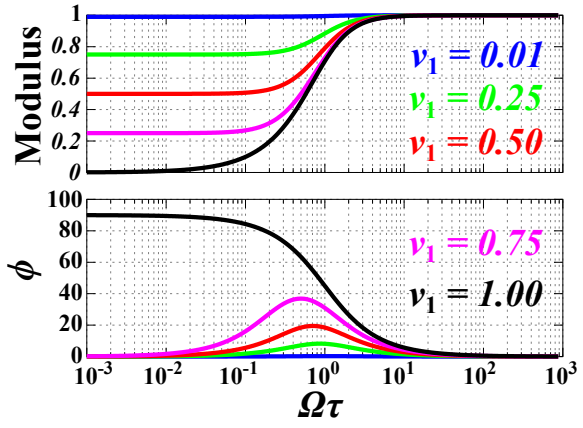

Figure 11: Non-dimensional loss modulus (top figure) and phase angle (bottom figure) for the Zener solid element versus non-dimensional frequency, $\Omega\tau$.

Comparing eqs. (23) and (27), the desired equivalence implies

$$G_e(\Omega) = E \approx E_0 \frac{(1-\nu_1) + (\Omega\tau)^2}{1 + (\Omega\tau)^2}, \tag{28a}$$

$$G_d(\Omega) = \Omega\eta \approx E_0 \frac{\nu_1(\Omega\tau)}{1 + (\Omega\tau)^2}. \tag{28b}$$

At low frequency, $\Omega\tau \ll 1$, the following conditions must hold: $E = E_0(1-\nu_1)$ and $\eta = E_0\nu_1\tau$. Clearly, the low frequency behavior of the Kelvin-Voigt and Zener solid elements will be nearly identical by selecting the following parameters of the Zener solid element: $E_0 = E/(1-\nu_1)$ and $\tau = (1-\nu_1)\eta/(\nu_1 E)$. Note that parameter ν_1 can be selected arbitrarily. A simple solution is obtained for $\nu_1 = 1/2$, leading to

$$E_\infty = E_1 = E, \tag{29a}$$

$$\tau = \frac{\eta}{E}. \tag{29b}$$

1.9 Viscoelastic branch properties definitions

As depicted in fig. 1, the generalized Maxwell model contains an elastic branch and N_b viscoelastic branches. The elastic branch properties are defined based on the classical elastic material constitutive law, while the viscoelastic branches properties are defined according to this section.

Each viscoelastic branch has two characteristic properties, a relaxation time τ_b and a characteristic stiffness matrix $\underline{\underline{\mathcal{D}}}_b$. Matrices $\underline{\underline{\mathcal{D}}}_b$ can be defined in different form according to the material symmetric types. The isotropic materials are considered here.

An isotropic material is a material that presents identical properties in all directions. For these materials, two independent parameters are needed to decide the stiffness matrix [1]. Because the shear behavior and bulk behavior are usually considered in viscoelasticity, the stiffness matrix defined here takes the following form,

$$E_b = \begin{bmatrix} (3\xi_b + 4\eta_b)/3 & (3\xi_b - 2\eta_b)/3 & (3\xi_b - 2\eta_b)/3 & 0 & 0 & 0 \\ (3\xi_b - 2\eta_b)/3 & (3\xi_b + 4\eta_b)/3 & (3\xi_b - 2\eta_b)/3 & 0 & 0 & 0 \\ (3\xi_b - 2\eta_b)/3 & (3\xi_b - 2\eta_b)/3 & (3\xi_b + 4\eta_b)/3 & 0 & 0 & 0 \\ 0 & 0 & 0 & \eta_b & 0 & 0 \\ 0 & 0 & 0 & 0 & \eta_b & 0 \\ 0 & 0 & 0 & 0 & 0 & \eta_b \end{bmatrix}. \tag{30}$$

Hence, for isotropic materials, the following three properties are required for each viscous branch: (1) Relaxation time: τ_b, (2) Bulk modulus: ξ_b, (3) Shear modulus: η_b.

These three required parameters can be obtained by material experiments. The time domain and the frequency domain experiments are introduced here.

1.10 Branch definitions in time domain

In time domain if a relaxation experiment in shear behavior is performed, according to equations (6) and (12), the time-dependent shear modulus becomes,

$$\eta(t) = \eta_\infty + \sum_{b=1}^{N_b} \eta_b e^{-t/\tau_b}, \tag{31}$$

where η_∞, which is time-independent, is the equivalent shear modulus defined in the elastic branch. Time-dependent shear modulus can be obtained by performing the relaxation experiment. The time-dependent shear modulus can then be approximated by a number of Prony series according to eq. (31), which can be fitted with the experiment data via different data fitting methods, such as least squares. Each Prony term is defined in one viscoelastic branch. In each branch the relaxation times for shear and bulk behavior are assumed to be identical. In fact, the relaxation times can usually be set in the experiments. The method to decide the bulk modulus in time domain is similar to that of shear modulus.

1.11 Branch definitions in frequency domain

In frequency domain if a dynamic mechanical analysis in shear behavior is performed, according to eq. (15), the shear response becomes,

$$\tau(t) = [\eta_e(\Omega) + i\eta_d(\Omega)]\,\gamma(t), \tag{32}$$

where $\gamma(t)$ is the harmonic shear strain, $\tau(t)$ is the shear stress response, $\eta_e(\Omega)$ is the storage shear modulus and $\eta_d(\Omega)$ is the loss shear modulus.

The absolute magnitude of the shear response is

$$|\tau| = \sqrt{\eta_e^2(\Omega) + \eta_d^2(\Omega)}|\gamma|, \tag{33}$$

and the phase lag of the shear response is

$$\phi = \arctan \frac{\eta_d(\Omega)}{\eta_e(\Omega)}. \tag{34}$$

Measurements of $|\tau|$ and ϕ obtained in the experiment can then be used to define η_e and η_d [4]. Then the storage shear modulus and loss shear modulus can be expressed parallel to eq. (17),

$$\eta_e(\Omega) = \eta_\infty + \sum_{b=1}^{N_b} \eta_b^* \frac{\Omega^2\tau_b^2}{1+\Omega^2\tau_b^2} \tag{35a}$$

$$\eta_d(\Omega) = \sum_{b=1}^{N_b} \eta_b^* \frac{\Omega\tau_b}{1+\Omega^2\tau_b^2}. \tag{35b}$$

In each branch the relaxation times for shear and bulk response are assumed to remain identical. The method for bulk behavior is also analogous to that of the shear behavior.

In general the three required parameters can be obtained from relaxation experiment according to eq. (31), or from harmonic dynamic mechanical analysis according to eq. (35).

2 Nonlinear viscoelasticity

The previous section has focused on the classical models of linear viscoelasticity. The accurate modeling of the behavior elastomeric materials, such as those found in aerospace applications, requires the development of nonlinear viscoelastic models. In this effort, the overall model consists of a number of branches all placed in parallel, as illustrated in fig. 12. Four types of branches will be used here: elastic branches, dashpot branches, plastic branches, Maxwell fluid branches, and viscous branches. The elastic branches consist of possibly nonlinear, elastic springs and the dashpot branches consist of possibly nonlinear, viscous dashpots. The Maxwell fluid branch is a linear branch that involves an internal state. The viscous and plastic branches are nonlinear and their behavior is modeled by differential equations involving additional internal states.

The total force generated by the device is the sum of the forces generated by the individual branches,

$$F = \sum F_e + \sum F_d + \sum F_p + \sum F_v, \qquad (36)$$

where F_e, F_d, F_p, and F_v are the forces in the elastic, dashpot, plastic and viscous branches, respectively. Any number of branches of each type can be used. Elastomers, especially carbon-black filled rubbers, exhibit complex constitutive behavior and the various branches of the proposed model each capture characteristic behavior of these materials.

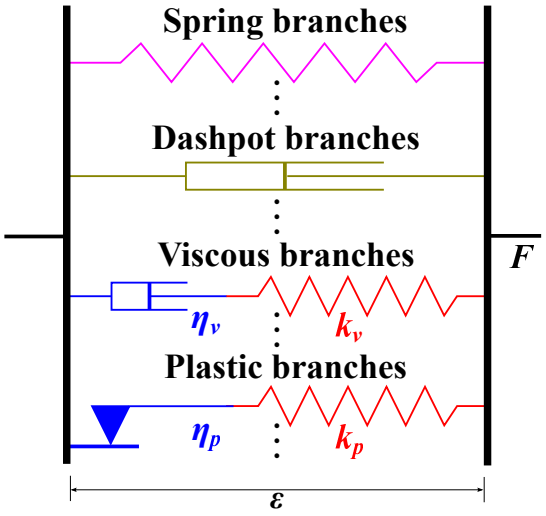

Figure 12: Configuration of the elastomeric device.

The total elongation of the device is denoted ϵ. Consequently, the elongations of the elastic and dashpot branches are both equal to that of the device. The viscous branches consist of a viscous and of an elastic component arranged in series; the elongations of these two components are denoted ϵ_v and ϵ_{ev}, respectively, such that $\epsilon = \epsilon_v + \epsilon_{ev}$. Similarly, the plastic branches consist of a plastic and of an elastic component arranged in series; the elongations of these two components are denoted ϵ_p and ϵ_{ep}, respectively, such that $\epsilon = \epsilon_p + \epsilon_{ep}$.

2.1 The elastic branch

The force in the elastic branch, denoted F_e, is a function of the elongation only, *i.e.*,

$$F_e = F_e(\epsilon). \qquad (37)$$

For a linear elastic spring, $F_e = k\epsilon$, where k is the elastic spring constant. For nonlinear elastic springs, eq. (37) can be recast as $F_e = k(\epsilon)\epsilon$, where the spring constant is now a function of the elongation.

2.2 The dashpot branch

The force in the dashpot branch, denoted F_d, is a function of the elongation rate only, *i.e.*,

$$F_d = F_d(\dot{\epsilon}). \qquad (38)$$

For a linear dashpot, $F_d = c\dot{\epsilon}$, where c is the dashpot constant. For nonlinear dashpots, eq. (38) can be recast as $F_e = c(\dot{\epsilon})\dot{\epsilon}$, where the dashpot constant is now a function of the elongation rate.

2.3 The plastic branch

The plastic branch consist of a plastic and of an elastic component arranged in series, as illustrated in fig. 13. The constitutive equation for the plastic branch is

$$\dot{F}_p = k_p \left(\dot{\epsilon} - \frac{|\dot{\epsilon}|}{\eta_p} F_p \right), \tag{39}$$

where F_p is the force in the plastic branch, $k_p > 0$ the stiffness constant of elastic part, and $\eta_p > 0$ a material parameters that characterizes the plastic behavior.

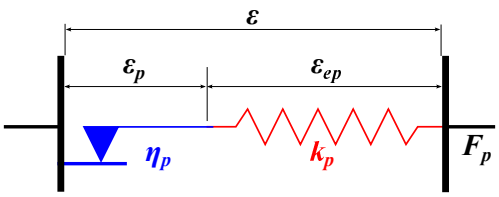

Figure 13: Configuration of the plastic branch.

2.4 The viscous branch

The viscous branch consist of a viscous and of an elastic component arranged in series, as illustrated in fig. 14. The generalized Maxwell model described in section 1.1 is a linear viscoelastic model consisting of a parallel arrangement for a single elastic branch and a number of Maxwell fluid branches, which are described in section 2.4.1. Because the viscous behavior of elastomeric materials is inherently nonlinear, various constitutive equations have been proposed to model their behavior. Two models will be described here, the Haupt-Sedlan and the Höfer-Lion models, described in sections 2.4.2 and 2.4.3, respectively.

2.4.1 The Maxwell fluid branch

Using the notation of fig. 14, the behavior of the Maxwell fluid branch is $F_v = \eta_v \dot{\epsilon}_v = k_v(\epsilon - \epsilon_v)$, where η_v and k_v are constants. These two equations are recast as

$$F_v = k_v(\epsilon - \epsilon_v), \tag{40a}$$

$$\tau_v \dot{\epsilon}_v + \epsilon_v = \epsilon, \tag{40b}$$

where $\tau_v = \eta_v / k_v$. Equation (40a) gives the force in the Maxwell fluid branch and eq. (40a) is the evolution equation for the internal state, ϵ_v. The model presents two parameters, τ_v and k_v. While this model describes the frequency-dependent properties of elastomeric materials adequately, it cannot represent their amplitude dependent behavior. Formulation (40) is identical to that developed earlier for linear viscoelasticity, see eq. (7). The parameters of the model are the relaxation time τ_v and k_v the stiffness constant of the spring.

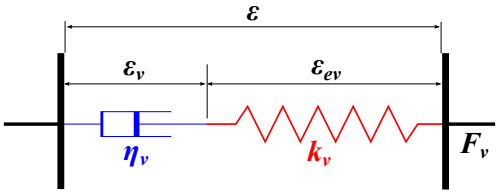

Figure 14: Configuration of the viscous branch.

Consider the evolution equation written as $\tau_v \dot{\alpha} + \alpha = \epsilon$. In practical implementations, a numerical solution of this equation will be required. Consider a typical time step: t_i and t_f are the initial and final times of the step and $h = t_f - t_i$ is the time step size. Let $\eta = (t - t_i)/h$ be the non-dimensional time within this time step and let $(\cdot)'$ denote a derivative with respect to η. The evolution equation now becomes $\alpha' + \bar{h}\alpha = \bar{h}\varepsilon(\eta)$, where $\bar{h} = h/\tau_v$ is the non-dimensional time step size.

Typically, the strain components are know at the beginning and the end of the time step: $\varepsilon(\eta) = \varepsilon_i + \eta(\varepsilon_f - \varepsilon_i)$, where ε_i and ε_f are the strain components at times t_i and t_f, respectively. For this linear evolution of the strain within a time step, the solution of eq. (41) is

$$\alpha(\eta) - \varepsilon(\eta) = (\alpha_i - \varepsilon_i) e^{-\bar{h}\eta} - (\varepsilon_f - \varepsilon_i) \frac{1 - e^{-\bar{h}\eta}}{\bar{h}}, \tag{41}$$

where $\alpha_i = \alpha(t_i)$. Finally, the value of the internal variable at the end of the time step, $\alpha_f = \alpha(t_f)$, is

$$\alpha_f - \varepsilon_f = (\alpha_i - \varepsilon_i)e^{-\bar{h}} - (\varepsilon_f - \varepsilon_i)\frac{1 - e^{-\bar{h}}}{\bar{h}}. \tag{42}$$

The initial state of the system is characterized by ε_i, the initial strain of the device, and α_i, the initial value of the internal state. Given the final value of the strain, ε_f, of the device, eq. (42) provides the final value of the internal state, α_f.

2.4.2 The Haupt-Sedlan branch

The viscous model proposed by Haupt and Sedlan [5] describes the behavior of the viscous branch in terms of two differential equations,

$$\dot{F}_v = k_v\dot{\epsilon} - \frac{(\xi z|\dot{\epsilon}| + 1)}{z}F_v, \tag{43a}$$

$$\dot{z}(t) = \frac{\sqrt{(z_{max} - z_{min})(z_{max} - z)}}{z_q} - \zeta(z - z_{min})|\dot{\epsilon}|, \quad z(0) = z_{max}, \tag{43b}$$

where F_v is the force in the viscous branch and z an internal state of the Haupt-Sedlan model. Equation (43a) is the governing equation for the viscous force; two material parameters appear in this equation, $k_v > 0$, the spring constant of the viscous branch and ξ. Equation (43b) is the evolution equation for the internal state that describes the evolution of relaxation time. This equation it involves four material parameters, z_{min}, z_{max}, z_q, and ζ. The initial condition for the evolution equation is $z(t = 0) = z_{max}$ and at all subsequent times, $z_{min} \leq z \leq z_{max}$. In practical implementations, a numerical solution of these nonlinear equations is required. It is convenient to use a Runge-Kutta [6] method for the integration process.

If $\zeta = 0$, the solution of eq. (43b) is $z = z_{max}$, *i.e.*, the internal state becomes constant, and eq. (43a) now reduces to

$$\dot{F}_v = k_v\dot{\epsilon} - \frac{(\xi z_{max}|\dot{\epsilon}| + 1)}{z_{max}}F_v. \tag{44}$$

This model involves three material parameters only: k_v, ξ, and z_{max}. If additionally $\xi = 0$, the model further degenerates into the Maxwell fluid element.

2.4.3 The Höfer-Lion branch

The viscous model proposed by Höfer and Lion [7] describes the behavior of the viscous branch in terms of three differential equations,

$$\dot{F}_v = k_v\dot{\epsilon} - \frac{\dot{z}}{\tau_0}F_v, \tag{45a}$$

$$\dot{z}(t) = \alpha\left(\bar{\tau}|\dot{\epsilon}| + 1\right) + (1 - \alpha)\left(\sum_{i=1}^{L} d_i q_i + 1\right), \tag{45b}$$

$$\dot{q}_i(t) = \frac{1}{\tau_{qi}}\left(\tau_{q0}|\dot{\epsilon}| - q_i\right), \quad i = 1, 2, \ldots L, \tag{45c}$$

where F_v is the force in the viscous branch, and z and q_i are internal states of the Höfer-Lion model. Equation (45a) is the governing equation for the viscous force; two material parameters appear in this equation, $k_v > 0$, the spring constant of the viscous branch and τ_0. Equation (45b) is the evolution equation for the internal state that describes the evolution of relaxation time. This equation it involves $2 + L$ material parameters, α, $\bar{\tau}$, and d_i, $i = 1, 2, \ldots L$. The initial condition

for the evolution equation is $z(t=0)=0$. Finally, each of the L internal states q_i, $i=1,2,\dots L$, has its own evolution behavior, as given by eqs. (45c). These equations involve $1+L$ additional material parameters, τ_{q0} and τ_{qi}, $i=1,2,\dots L$.

The two terms in the right-hand side of eq. (45b) were proposed for different purposes. The first term describes the short-term behavior of the material between amplitude steps, while the second term is included to describe the long-term recovery behavior of the elastic modulus.

When $\alpha=1$, eq. (45b) reduces to $\dot{z}(t)=\bar{\tau}|\dot{\epsilon}|+1$, and the additional internal states, q_i, $i=1,2,\dots L$, no longer affect device response. Furthermore, eq. (45b) then becomes identical to eq. (44), provided that $\xi=\bar{\tau}/\tau_0$ and $z_{max}=\tau_0$. Clearly, for $\alpha=1$, the Höfer and Lion model is a particular case of the Haupt-Sedlan model, and hence, in the following, case $\alpha=0$ only is developed.

2.4.4 The simplified Höfer-Lion case

For $\alpha=0$, the Höfer-Lion model characterized by eqs. (45) and eq. (45c) into eq. (45a) yields,

$$\dot{F}_v = k_v\dot{\epsilon} - \frac{\sum_{i=1}^{L} d_i q_i + 1}{\tau_0} F_v, \tag{46a}$$

$$\dot{q}_i = \frac{1}{\tau_{qi}}\left(\tau_{q0}|\dot{\epsilon}| - q_i\right), \quad i=1,2,\dots L, \tag{46b}$$

where k_v is the stiffness of the elastic part and τ_0 is the constant relaxation time. Each internal state q_i introduces two material parameters, d_i and τ_{qi}. The internal states describe the amplitude dependence of material behavior. A constant $\tau_{q0}=1$ sec is introduced for dimensional reasons. In practical implementations, a numerical solution of these nonlinear equations is required. It is convenient to use a Runge-Kutta [6] method for the integration process.

When all d_i vanish, the simplified Höfer-Lion further degenerates into the Maxwell fluid element model, stated as $\dot{F}_v = k_v\dot{\epsilon} - F_v/\tau_0$.

References

[1] L.E. Malvern. *Introduction to the Mechanics of a Continuous Medium.* Prentice Hall, Inc., Englewood Cliffs, New Jersey, 1969.

[2] R.M. Christensen. *Theory of Viscoelasticity. An Introduction.* Academic Press, New York and London, second edition, 1982.

[3] J.C. Simo and T.J.R. Hughes. *Computational Inelasticity.* Springer, New York, Berlin, Heidelberg, 1998.

[4] *Abaqus Theory Manual, Abaqus Version 6.7 edition.*

[5] P. Haupt and K. Sedlan. Viscoplasticity of elastomeric materials: Experimental facts and constitutive modeling. *Archive of Applied Mechanics*, 71(5):89–109, 2001.

[6] W.H. Press, S.A. Teutolsky, W.T. Vetterling, and B.P. Flannery. *Numerical Recipes. The Art of Scientific Computing.* Cambridge University Press, Cambridge, third edition, 2007.

[7] P. Höfer and A. Lion. Modeling of frequency- and amplitude-dependent material properties of filler-reinforced rubber. *Journal of the Mechanics and Physics of Solids*, 57(4):500–520, 2009.